PHYSICAL REVIEW B VOLUME 36, NUMBER 11 15 OCTOBER 1987-I

# Electronic structure of $Pb_{1-x}Sn_xTe$ semiconductor alloys

Seongbok Lee and John D. Dow
*Department of Physics, University of Notre Dame, Notre Dame, Indiana 46556*
(Received 20 April 1987)

The electronic structures of the pseudobinary alloy semiconductors $Pb_{1-x}Sn_xTe$ are analyzed using a tight-binding model with spin-orbit interaction. The densities of states and the band gaps at the $L$ point are computed for both the effective media using the virtual-crystal approximation and the realistic media employing the recursion method, and the results are compared. Both theories exhibit alloying effects such as band broadening, energy shifts, and Dimmock's band-crossing phenomenon. However, significant deviations from the virtual-crystal approximation are found for the cation-derived $s$-like deep valence-band states.

## I. INTRODUCTION

The narrow-gap IV-VI semiconductor compounds and their pseudobinary alloys have unique properties. They have on the average five valence electrons per atom, small direct band gaps at the $L$ point, and high static dielectric constants of order $10^3$. They often show a variety of anomalous thermodynamic, acoustic, and electronic properties.[1,2] $Pb_{1-x}Sn_xTe$ is an especially interesting semiconductor alloy because the symmetry of valence- and conduction-band edges of SnTe is reversed compared to PbTe and other IV-VI semiconductors: The conduction- and the valence-band edges have $L_6^-$ and $L_6^+$ symmetry, respectively, in PbTe and most other IV-VI semiconductors, while the ordering is "Dimmock reversed" in SnTe.[1-3] This has an interesting consequence: the fundamental band gap closes to zero at an intermediate composition $x$ in $Pb_{1-x}Sn_xTe$.[3] This property of the fundamental energy-band gap vanishing for a selected composition means that alloys with compositions near this composition exhibit small band gaps that satisfy the special needs for infrared sources[4] and detectors[5] in modern technology. Therefore it is very important to understand the effects of alloy disorder on the electronic structures of these technologically important materials.

Recently, Spicer *et al.*[6] have reported experiments indicating the selective breakdown of the virtual-crystal approximation for deep valence bands in $Hg_{1-x}Cd_xTe$ [which is a covalent semiconductor alloy containing "light" (Cd) and "heavy" (Hg) atoms], and have identified that phenomenon as resulting from the Hg $6s$ atomic levels being significantly below the Cd $5s$ levels. Also, Hass *et al.*[7] have obtained similar disorder effects theoretically, in $Hg_{1-x}Cd_xTe$ using the coherent-potential approximation. Davis[8] has also found large deviations from virtual-crystal behavior theoretically in $Pb_{1-x}Sr_xS$ where the cations Pb (configuration $6s^26p^2$) and Sr (configuration $5s^2$) differ so much that an average cation potential is meaningless.

The present work analyzes the effects of alloy disorder on the electronic structures of the random alloys $Pb_{1-x}Sn_xTe$ using the recursion method with a tight-binding model. $Pb_{1-x}Sn_xTe$ is an interesting material for this purpose because its constituent semiconductor compounds PbTe and SnTe have very similar overall electronic structures, except for the Dimmock reversal of the valence- and conduction-band edges; the alloy contains light (Sn) and heavy (Pb) cations. Moreover, the electronic band structures of these materials have large spin-orbit splittings, and the fundamental gaps are not at the center of the Brillouin zone, $\mathbf{k}=\mathbf{0}$. Indeed, some authors believe that PbTe and SnTe are ionic rather than covalent materials.[9] Therefore the usual criteria[10] for the validity of the virtual-crystal approximation may not apply.

In Sec. II, the tight-binding model for the parent semiconductors PbTe and SnTe is discussed, and the recursion method is outlined. In Sec. III, the results of the calculations are presented and discussed. Section IV summarizes the conclusions.

## II. CALCULATIONAL PROCEDURES

### A. Tight-binding model

It is well known that $Pb_{1-x}Sn_xTe$ forms a single-phase pseudobinary alloy over the entire composition range $x$, with about 2% of lattice-constant change from PbTe to SnTe. Both compounds crystallize in the rock-salt structure with lattice constant 6.443 Å for PbTe and 6.327 Å for SnTe (Ref. 11) at 300 K. The electronic structures of PbTe and SnTe (and other IV-VI compounds) have been extensively investigated theoretically and experimentally.[1,2] A variety of computational techniques such as the relativistic augmented-plane-wave (APW) method,[12-14] the orthonormalized-plane-wave (OPW) method,[15] the empirical pseudopotential method,[16-19] and the relativistic Green's function or Korringa-Kohn-Rostoker method (KKR) (Ref. 20) have been used to calculate the electronic band structures of these materials. More recently, a self-consistent relativistic APW calculation for SnTe (Ref. 21) and first-principles pseudopotential total-energy calculation for

 

the ground-state properties and electronic structures of PbTe and SnTe (Ref. 22) have been reported. Although considerable differences may exist concerning some details, such as the parity assignments at the $L$ point[23] and gap structures at critical points (for example, some calculations[13,16,21] showed a "hump structure," i.e., the $L$ point is not a minimum- or maximum-energy point, but a saddle point in SnTe), the general features of the various band structures mentioned above are quite similar. Concentrating on this point and the fact that the recursion method takes its most convenient form in a tight-binding model, we shall use in this work the empirical tight-binding Hamiltonian matrix elements of Lent *et al.*,[24] which are obtained by fitting the eigenvalues of the tight-binding Hamiltonian matrix to the experimental band gap at the $L$ point and to band energies at symmetry points, as calculated by Herman *et al.*[15]

Since the relativistic corrections to the energies of heavy materials, particularly those including Pb, are significant,[25,26] the Hamiltonian used for band calculations should include these effects. The relativistic Hamiltonian which produces the energy-band structure has the following form:[12]

$$H=(p^2/2m)+V+H_{\rm so}+\hbar^2\nabla^2V/8m^2c^2-p^4/8m^3c^2 , \tag{1}$$

where $V$ is the periodic crystal potential. The spin-orbit term which may split degenerate levels is

$$H_{\rm so}=\hbar\boldsymbol{\sigma}\cdot(\nabla\times\mathbf{p})/4m^2c^2 , \tag{2}$$

and the remaining terms are the Darwin and mass-velocity terms, respectively.

Employing the ideas of Harrison,[27] Chadi,[28] and Vogl *et al.*,[29] the nearest-neighbor tight-binding Hamiltonian can be constructed,

$$\begin{aligned}H_0=&\sum_{\mathbf{R},\sigma,i}(\,|\,a,i,\sigma,\mathbf{R}\rangle E_{i,a}\langle a,i,\sigma,\mathbf{R}\,|\\&+|\,c,i,\sigma,\mathbf{R}+\mathbf{d}\rangle E_{i,c}\langle c,i,\sigma,\mathbf{R}+\mathbf{d}\,|\,)\\&+\sum_{\mathbf{R},\mathbf{R}',\sigma,i,j}(\,|\,a,i,\sigma,\mathbf{R}\rangle V_{i,j}\langle c,j,\sigma,\mathbf{R}'+\mathbf{d}\,|\\&+\text{H.c.})+H_{\rm so} ,\end{aligned} \tag{3}$$

where H.c. means Hermitian conjugate, $\mathbf{R}$ are the lattice vectors, $i$ and $j$ are the localized quasiatomic orbitals for the cation and anion, $\sigma$ is the spin index (up or down), $a$ and $c$ refer to the anion and cation, respectively, and $\mathbf{d}$ is the position of the cation relative to the anion in any unit cell: $\mathbf{d}=(a_L/2,0,0)$. The spin-orbit interaction term can be described by the following Hamiltonian:[24]

$$H_{\rm so}=\sum_{\mathbf{R},i,j,\sigma,\sigma'}[\,|\,a,i,\sigma,\mathbf{R}\rangle(\lambda_a/2)\mathbf{L}_a\cdot\boldsymbol{\sigma}_a\langle a,j,\sigma',\mathbf{R}\,|+|\,c,i,\sigma,\mathbf{R}\rangle(\lambda_c/2)\mathbf{L}_c\cdot\boldsymbol{\sigma}_c\langle c,j,\sigma',\mathbf{R}\,|\,] . \tag{4}$$

As a basis set, we used 18 quasiatomic orbitals localized on each atomic site which are assumed to be mutually orthonormalized by the method of Löwdin:[30] $s$, $p_x$, $p_y$, $p_z$, $d_{x^2-y^2}$, $d_{3z^2-r^2}$, $d_{xy}$, $d_{yz}$, and $d_{zx}$ for each spin-up and -down state. The parameters of this model are given in Ref. 24, and reproduce the experimental band gaps at the $L$ point[3] (0.186 eV for PbTe and 0.3 eV for SnTe) as well as the calculated band energies of Ref. 15 at the high-symmetry points $\Gamma$, $X$, and $L$. The resulting band structures are given in Ref. 24. In particular, the Dimmock reversal of the band structure from PbTe to SnTe is correctly reproduced by the model.

### B. Recursion method

To obtain the densities of states of $Pb_{1-x}Sn_xTe$ alloys, we require a theory that is capable of predicting the spectra characteristic of pairs and clusters of minority atoms, namely a theory that goes beyond the virtual-crystal approximation (VCA) (Ref. 31) and the coherent-potential approximation (CPA) (Refs. 6, 7, 10, and 32–36). We use the recursion method,[8,37] which exploits the fact that the Hamiltonian matrix for the alloy can be transformed into a real symmetric matrix by unitary transformation from the old basis $|\,\xi\rangle$ (with $\xi=0,1,\ldots,N$, where $\xi$ stands for $b,i,\sigma,\mathbf{R}$) to a new basis $|\,\nu\}$ ($\nu=0,1,2,\ldots,N$). Thus we have

$$H\,|\,\nu\}=b_\nu\,|\,\nu-1\}+a_\nu\,|\,\nu\}+b_{\nu+1}\,|\,\nu+1\} . \tag{5}$$

With an initial choice of $|\,0\}$ and $b_0=0$, this equation can be iterated to determine the recursion coefficients $a_\nu$ and $b_\nu$ ($\nu=0,1,\ldots,N$) and the Green's function:

$$G_{0,0}(E)=\cfrac{1}{E-a_0-\cfrac{b_1^2}{E-a_1-\cfrac{b_2^2}{E-a_2-\cdots}}} , \tag{6}$$

where $E$ has an infinitesimal positive imaginary part. In practice this expansion is cut off at some finite level $L$ ($=51$ here), and the remainder is neglected. Then the local densities of states for a specific site $b$ and symmetries $i$ are obtained from $G_{0,0}$ by taking the imaginary part: $(-1/\pi)\mathrm{Im}G_{0,0}$. The choice of initial state $|\,0\}$,

$$|\,0\}=\sum_{\mathbf{R},\sigma}\pm\,|\,b,i,\sigma,\mathbf{R}\rangle , \tag{7}$$

where $\pm$ means that each term is given a randomly chosen sign, yields the local density of states projected onto the $b$ (anion or cation) site and the symmetry $i$ in a random alloy, and the sum of these local-state densities is the total density of states. Details of the method can be found in Ref. 37; computer programs for executing the recursion method are available.[38]

## III. RESULTS AND DISCUSSION

We first calculate the density of states for the perfect crystals PbTe and SnTe, employing the nearest-neighbor tight-binding model discussed in the previous section. The results are shown in Figs. 1 and 2. The dot-dashed curve is the density of states obtained by the Lehmann-Taut method.[39] In this method, the Brillouin zone is decomposed into a set of tetrahedra, and the integration over the Brillouin zone is evaluated using an analytic expression. The solid curve is from the recursion method. A $12\times12\times12$-atom cluster was generated to simulate the perfect infinite crystal, and the local density of states for each orbital $i,\sigma$ was calculated with periodic boundary conditions.

The overall agreement between the two methods is very good, except for some minor details such as the peak structures and the band-gap smearing; the differences between the results of the recursion method and the Lehmann-Taut method are within the tolerable range. The $\delta$-function-like peaks are associated with van Hove singularities[40] due to the long-range order. The more or less smooth peaks in the upper valence bands given by the recursion method (solid curve) are partly due to the finite size of the cluster and partly due to the limited resolution of the present method because of the finite cutoff at $L=51$. (We determined this by varying the size of the cluster and $L$.) Another difference is that while the Lehmann-Taut method clearly shows the band gap to contain no states, the band edges are smeared in the recursion method. The main reasons for this are the limited resolution of the method and the incomplete cancellation of the off-diagonal elements of the Green's function due to the choice of randomly phased initial state. The band edges can be sharpened by choosing an initial state $|0\}$ localized at the center of a cluster or by investigating the spectral density of states (as will be discussed below). In Fig. 3, the contribution of each orbital

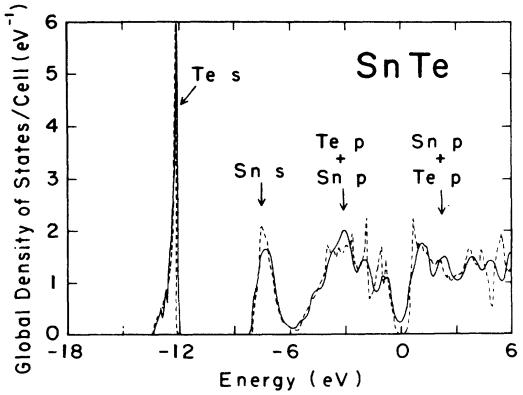


FIG. 2. The virtual-crystal-approximation (dot-dashed curve) and the recursion-method (solid curve) density of states in SnTe. A $12\times12\times12$-atom cluster with periodic boundary conditions was used in the recursion method.

to the density of states of PbTe is displayed. The lowest valence band is predominantly anion $s$-like, and the middle valence band is cation $s$-like. The upper valence bands have dominant anion $p$-like character, while the lower conduction bands are $p$-like and cation derived. This can be visualized by the following simple picture. The Pb atom has four valence electrons ($6s^26p^2$) with free-atomic orbital energies $-12.42$ and $-6.95$ eV (relative to vacuum) for $s$ and $p$ orbitals, respectively, and the Te atom has six valence electrons ($5s^25p^4$) with orbital energies $-19.05$ eV ($5s$) and $-9.79$ eV ($5p$).[41] The two $5s$ electrons of Te, which have the lowest orbital energies, form an isolated valence band deep in energy, and the two $6s$ electrons of Pb form a middle valence band. The two $6p$ electrons of Pb and the four $5p$ electrons of Te interact with each other to form bonding (valence band) and antibonding (conduction band) bands. There-

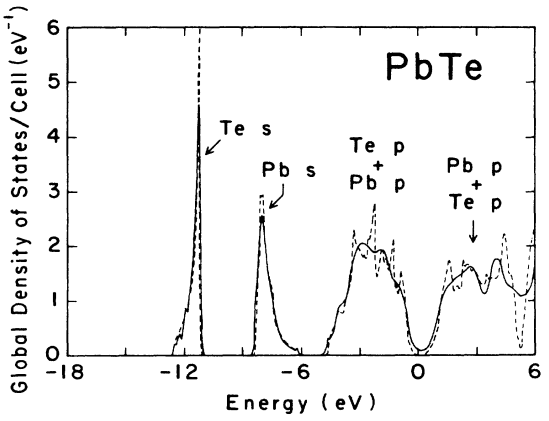


FIG. 1. The virtual-crystal-approximation (dot-dashed curve) and the recursion-method (solid curve) density of states in PbTe. A $12\times12\times12$-atom cluster with periodic boundary conditions was used in the recursion method. The zero of energy is the valence-band maximum.

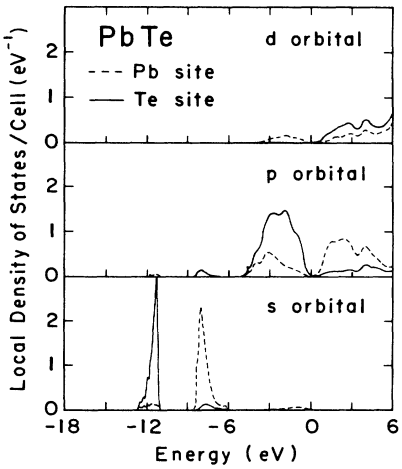


FIG. 3. Local density of states for cation (dot-dashed curve) and anion (solid curve) calculated by the recursion method in PbTe.

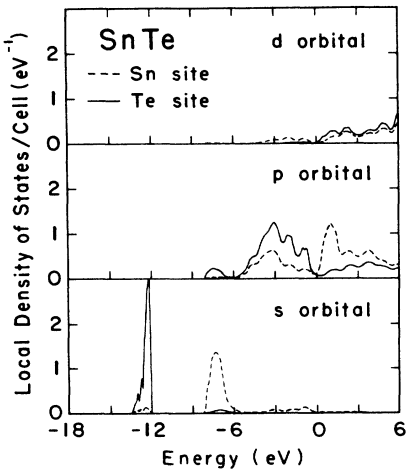


FIG. 4. Local density of states for cation (dot-dashed curve) and anion (solid curve) calculated by the recursion method in SnTe.

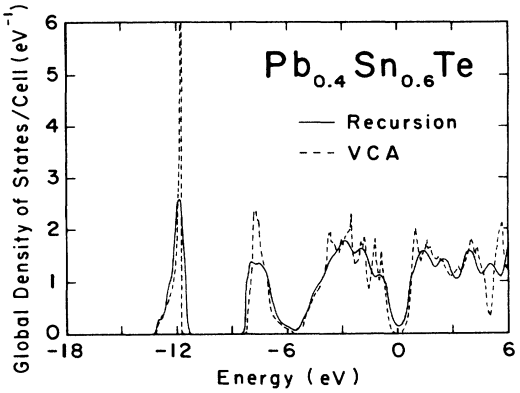


FIG. 6. The virtual-crystal-approximation (dot-dashed curve) and the recursion-method (solid curve) density of states in $Pb_{0.4}Sn_{0.6}Te$. A $12\times12\times12$-atom cluster with periodic boundary conditions was used in the recursion method.

fore, alloying PbTe and SnTe, which is equivalent to distributing Pb and Sn atoms randomly on cation sites, has the largest effect on the cationlike middle valence band. The characteristics of the local density-of-states structure in SnTe are similar to those of PbTe (see Fig. 4); the $5s$ and $5p$ free-atomic orbital energies of Sn are at $-12.97$ and $-7.21$ eV, respectively.

We generate a model of the random alloy $Pb_{1-x}Sn_xTe$ by randomly occupying cation sites by either Pb (with probability $1-x$) or Sn (with probability $x$), while all anion sites are occupied by Te. The matrix elements of the alloy Hamiltonian are derived from those of PbTe and SnTe as follows: On cation sites, we use either PbTe or SnTe matrix elements, depending on whether the site was occupied by Pb or Sn. On Te sites, we average the PbTe and SnTe matrix elements, weighting the average in proportion to the number of neighboring Pb and Sn atoms to the Te. Then the densities of states for $Pb_{1-x}Sn_xTe$ are calculated using both the virtual-crystal approximation and the recursion method for a number of compositions $x$. Again, the density of states is obtained by the use of the Lehmann-Taut method in the virtual-crystal approximation, and a $12\times12\times12$-atom cluster is used in the recursion method with periodic boundary conditions. In order to avoid sample-dependent results, we repeated the calculations for five different alloy configurations of $12^3$ atoms, and averaged the densities of states. The results are shown in Figs. 5–8. The solid curves represent the recursion density of states, and the dot-dashed curves are for the virtual-crystal approximation (VCA) results. Both the virtual-crystal approximation and the recursion density of states show the alloying effects, i.e., energy shifts and width changes of the density-of-states peaks. However, analysis of the middle valence band near $-7$ eV, which has the greatest alloying effects, clearly reveals the differences between the predictions of the two

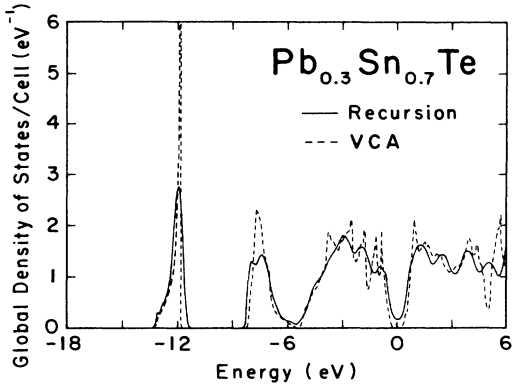


FIG. 5. The virtual-crystal-approximation (dot-dashed curve) and the recursion-method (solid curve) density of states in $Pb_{0.3}Sn_{0.7}Te$. A $12\times12\times12$-atom cluster with periodic boundary conditions was used in the recursion method.

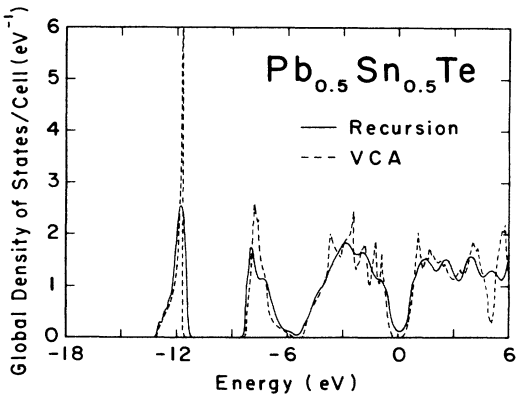


FIG. 7. The virtual-crystal-approximation (dot-dashed curve) and the recursion-method (solid curve) density of states in $Pb_{0.5}Sn_{0.5}Te$. A $12\times12\times12$-atom cluster with periodic boundary condition was used in the recursion method.

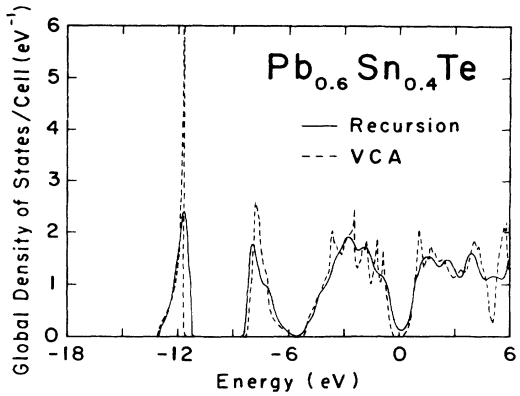


FIG. 8. The virtual-crystal-approximation (dot-dashed curve) and the recursion-method (solid curve) density of states in $Pb_{0.6}Sn_{0.4}Te$. A $12\times12\times12$-atom cluster with periodic boundary condition was used in the recursion method.

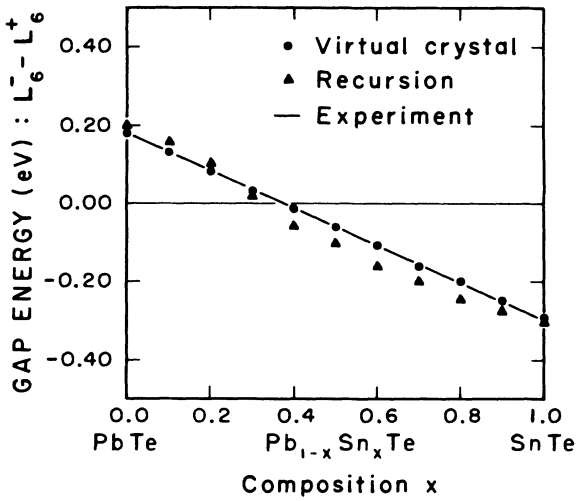


FIG. 9. The band gap $E(L_6^-)-E(L_6^+)$ of $Pb_{1-x}Sn_xTe$ vs composition $x$. The solid circles (triangles) are obtained using the virtual-crystal approximation (the recursion method), and the solid line represents the interpolation of PbTe and SnTe experimental results of Ref. 3.

methods—the effect of disorder. This band is a doublet, with its low- and high-energy components due to Pb and Sn $s$ states, respectively.

Since the bands that exhibit the alloy effects which are beyond the virtual-crystal approximation are cation $s$-like in character, spin-orbit coupling does not produce any novel features in the spectra of $Pb_{1-x}Sn_xTe$, beyond the spin-orbit features found in PbTe, SnTe, and a virtual-crystal theory of $Pb_{1-x}Sn_xTe$.

Fortunately the results we find agree rather well with what is expected, based on the Onodera-Toyozawa theory of alloys[10]—despite the fact that theory, to our knowledge, has not been applied previously to alloys with fundamental band gaps at the $L$ point of the Brillouin zone. The density-of-states spectra of the alloys exhibit some features that are "persistent" and others that are "amalgamated" in the terminology of Ref. 10. The persistent features are associated with the cationlike middle valence bands: the Pb $6s$-like and Sn $5s$-like bands that retain their characters in the alloy because the perfect-crystal bands do not overlap in energy. The remaining bands are amalgamated and tend to form hybrids of the PbTe and SnTe bands rather than exhibit separate PbTe- and SnTe-like bands. This amalgamation occurs because the PbTe and SnTe bands overlap in energy, and hence mix in the alloy.[10] Bands that fall within this amalgamated regime can generally be described, in a first approximation, by the virtual-crystal approximation.

Although it is straightforward to include a valence-band offset in the calculation by adding a constant energy to all of the diagonal matrix elements of either PbTe or SnTe (by construction, the matrix elements of Ref. 24 place the zero of energy at the valence-band maximum), we have not done so here because the offset is thought to be small (of order 60 meV),[42] almost negligible on the scale of the figures.

It is well-known that the fundamental band gap of $Pb_{1-x}Sn_xTe$ closes at some intermediate composition because of the inverted band structure of SnTe. We calculated $E(L_6^-)-E(L_6^+)$ of $Pb_{1-x}Sn_xTe$ as a function of composition $x$ by diagonalizing the virtual-crystal empirical tight-binding Hamiltonian (solid circles in Fig. 9). Also the corresponding quantity can be calculated using the recursion method. In alloys, the translational symmetry is broken, thus the wave vector $\mathbf{k}$ is not a good quantum number. However, we still can define the spectral-density functions analogous to those of the perfect crystal by the following:[8]

$$A(\mathbf{k},E)=-(1/\pi)\lim_{\epsilon\to0}\mathrm{Im}\langle b,i,\sigma,\mathbf{k}\,|\,G(E+i\epsilon)\,|\,b,i,\sigma,\mathbf{k}\rangle, \tag{8}$$

where $|\,b,i,\sigma,\mathbf{k}\rangle$ is a normalized Bloch sum over all unit cells of orbital $i$ with spin $\sigma$ on each atomic site $b$ (anion or cation). Then the position and broadening of the peak represents the energy shift and damping of a particular quasiparticle state of energy $E$ and wave vector $\mathbf{k}$. Since $L_6^+$ ($L_6^-$) has anion (cation) $p$-like character, a Bloch sum of $(p_x+p_y+p_z)/\sqrt{3}$ on each anion (cation) site at the $L$ point is chosen as the initial state $|\,0\rangle$ for $L_6^+$ ($L_6^-$), and the spectral density of states $A(\mathbf{k},E)$ is calculated. Then the gap is defined by the differences in the peak values of $A(\mathbf{k},E)$, i.e., $E(L_6^-)-E(L_6^+)$. The theoretical predictions are shown also in Fig. 9 (solid triangles) in comparison with a linear interpolation of the experimental band gaps of PbTe and SnTe (Ref. 3) (solid line). The theoretical uncertainty in $E(L_6^-)-E(L_6^+)$ is $\sim\pm0.02$ eV for $0<x<1$. The calculated band gap is almost a linear function of composition $x$ and compares well with the experimental results.

## IV. SUMMARY

The electronic structures of $Pb_{1-x}Sn_xTe$ alloys, including their parent semiconductor compounds, have

been analyzed using the tight-binding model with spin-orbit interaction. The densities of states were computed for both the effective media using the virtual-crystal approximation and the realistic media employing the recursion method, and the results were compared. As expected, both theories exhibited alloying effects such as band broadening and energy shifts. However, the two methods differed in their predictions for the cation-derived $s$-like states, which experienced the greatest alloying effect. The alloy composition dependence of the band gap at the $L$ point was analyzed, and exhibits Dimmock's band-crossing phenomenon. The above facts show that the recursion method is a useful tool for the study of the electronic structure of random $Pb_{1-x}Sn_xTe$, and in particular for the cationlike middle valence band. However, they also show that the virtual-crystal approximation provides a remarkably good description of the electronically important top valence and bottom conduction bands. Finally, they demonstrate that the Onodera-Toyozawa criteria can be applied to $Pb_{1-x}Sn_xTe$, even though these alloys have their fundamental band gaps at $L$: the cationlike $s$-like middle valence bands are persistent while the top valence band and lowest conduction band are amalgamated.

## ACKNOWLEDGMENTS

We are grateful to the Office of Naval Research (Contract No. N00014-84-K-0352), the Air Force Office of Scientific Research (Contract No. AFOSR-85-0331), the University of Notre Dame, and the University of Illinois at Urbana-Champaign Physics Department for their support of this work. We benefited greatly from stimulating conversations with M. Bowen, E. Ho, C. Lent, and O. Sankey.

[1]W. Jantsch, in *Dynamical Properties of* IV-VI *Compounds*, Vol. 99 of *Springer Tracts in Modern Physics* (Springer-Verlag, Berlin, 1983), p. 1; A. Bussmann-Holder, H. Bilz, and P. Vogl, *ibid.*, p. 51.

[2]G. Nimiz and B. Schlicht, in *Narrow-Gap Semiconductors*, Vol. 98 of *Springer Tracts in Modern Physics* (Springer-Verlag, Berlin, 1983), p. 1.

[3]J. O. Dimmock, I. Melngailis, and A. J. Strauss, Phys. Rev. Lett. **16**, 1193 (1966).

[4]H. Preier, Appl. Phys. **20**, 189 (1979).

[5]H. Holloway, J. Appl. Phys. **50**, 1386 (1979).

[6]W. E. Spicer, J. A. Silberman, M. Morgan, I. Lindau, J. A. Wilson, A.-B. Chen, and A. Sher, Phys. Rev. Lett. **49**, 948 (1982).

[7]K. C. Hass, H. Ehrenreich, and B. Velický, Phys. Rev. B **27**, 1088 (1983).

[8]L. C. Davis, Phys. Rev. B **28**, 6961 (1983).

[9]M. Schlüter, G. Martinez, and M. L. Cohen, Phys. Rev. B **11**, 3808 (1975).

[10]Y. Onodera and Y. Toyozawa, J. Phys. Soc. Jpn. **24**, 341 (1968).

[11]R. F. Bis and J. R. Dixon, J. Appl. Phys. **40**, 1918 (1969).

[12]J. B. Conklin, L. E. Johnson, and G. W. Pratt, Phys. Rev. **137**, A1282 (1965).

[13]S. Rabii, Phys. Rev. **182**, 821 (1969).

[14]S. Rabii and R. H. Lasseter, Phys. Rev. Lett. **33**, 703 (1974).

[15]F. Herman, R. L. Kortum, I. B. Ortenberg, and J. P. van Dyke, J. Phys. (Paris) Colloq. **29**, C4-62 (1968).

[16]Y. W. Tung and M. L. Cohen, Phys. Rev. **180**, 823 (1969).

[17]R. L. Bernick and L. Kleinman, Solid State Commun. **8**, 569 (1970).

[18]S. E. Kohn, P. Y. Yu, Y. Petroff, Y. R. Shen, Y. Tsang, and M. L. Cohen, Phys. Rev. B **8**, 1477 (1973).

[19]G. Martinez, M. Schlüter, and M. L. Cohen, Phys. Rev. B **11**, 651 (1975).

[20]H. Overhof and U. Rössler, Phys. Status Solidi **37**, 691 (1970); J. Korringa, Physica **13**, 392 (1947); W. Kohn and N. Rostoker, Phys. Rev. **94**, 1111 (1954).

[21]J. S. Melvin and D. C. Hendry, J. Phys. C **12**, 3003 (1979).

[22]K. M. Rabe and J. D. Joannopoulos, Phys. Rev. B **32**, 2302 (1985).

[23]See for example, G. Martinez and M. L. Cohen, Phys. Rev. Lett. **35**, 1746 (1975), and references therein.

[24]C. S. Lent, M. A. Bowen, J. D. Dow, R. S. Allgaier, O. F. Sankey, and E. S. Ho, Superlatt. Microstruct. **2**, 491 (1986).

[25]L. E. Johnson, J. B. Conklin, and G. W. Pratt, Phys. Rev. Lett. **11**, 538 (1963).

[26]F. Herman, C. D. Kuglin, K. F. Cuff, and R. L. Kortum, Phys. Rev. Lett. **11**, 541 (1963).

[27]W. A. Harrison, Phys. Rev. B **8**, 4487 (1973).

[28]D. J. Chadi, Phys. Rev. B **16**, 790 (1977).

[29]P. Vogl, H. P. Hjalmarson, and J. D. Dow, J. Phys. Chem. Solids **44**, 365 (1983).

[30]P.-O. Lödin, J. Chem. Phys. **17**, 365 (1950).

[31]L. Northeim, Ann. Phys. (N.Y.) **9**, 607 (1931); **9**, 641 (1931); F. Bassani and D. Brust, Phys. Rev. **131**, 1524 (1963); H. Amar, K. H. Johnson, and C. B. Sommers, *ibid.* **153**, 655 (1967); M. M. Pant and S. K. Joshi, *ibid.* **184**, 635 (1969).

[32]P. Soven, Phys. Rev. **156**, 809 (1967).

[33]D. W. Taylor, Phys. Rev. B **15**, 1017 (1967).

[34]B. Velický, S. Kirkpatrick, and H. Ehrenreich, Phys. Rev. **175**, 747 (1968).

[35]A.-B. Chen and A. Sher, Phys. Rev. B **17**, 4726 (1978).

[36]A.-B. Chen and A. Sher, Phys. Rev. B **23**, 5360 (1981).

[37]R. Haydock, in *Solid State Physics*, edited by H. Ehrenreich, F. Seitz, and D. Turnbull (Academic, New York, 1980), Vol. 35, p. 215.

[38]S. Lee, Ph.D. thesis, University of Illinois at Urbana-Champaign, 1986 (unpublished).

[39]G. Lehmann and M. Taut, Phys. Status Solidi B **54**, 469 (1972).

[40]L. van Hove, Phys. Rev. **89**, 1189 (1953).

[41]C. F. Fisher, At. Data **4**, 301 (1972).

[42]K. E. Ambrosch, H. Clemens, E. J. Fantner, G. Bauer, M. Kriechbaum, P. Kocevar, and R. J. Nicholas, Surf. Sci. **142**, 571 (1984).